

SPH model to simulate Oscillating Water Column wave energy converter

C. Altomare, T. Suzuki
Flanders Hydraulic Research
Antwerp, Belgium
corrado.altomare@mow.vlaanderen.be,
tomohiro.suzuki@mow.vlaanderen.be

A.J.C. Crespo, J.M. Domínguez, A. Barreiro,
J. González-Cao and M. Gómez-Gesteira
EPHYSLAB, Universidade de Vigo
Ourense, Spain
alexbexe@uvigo.es, jmdominguez@uvigo.es,
anxo.barreiro@uvigo.es, jgcao@uvigo.es
mggesteira@uvigo.es

Abstract— The DualSPHysics code is applied to simulate the interaction between sea waves and an Oscillating Water Column device (OWC). The model is first validated with laboratory tests where oscillations of the water surface inside a fixed OWC chamber are compared with results from a time-domain model, mesh-based solutions and experiments. The capabilities of the model are then demonstrated by simulating a floating offshore OWC moored to the seabed.

I. INTRODUCTION

Significant research is being conducted into renewable resources due to the increasing demand for energy and to the uncertainty related to climate change and increasing storminess. Wave energy is one of the most available and cleanest renewable energy sources. Wave energy has in fact the advantage of being considered as the most concentrated and least variable form of renewable energy.

Oscillating water column (OWC) devices consist of a partially submerged reservoir with water open to the sea and a chamber of trapped air. The ocean waves change the water level inside the tank, which compresses and decompresses the

air inside the chamber. This trapped air is allowed to flow to and from the atmosphere via a turbine whose rotation is used to generate electricity. The shoreline OWC's are currently the most sensible designs since they do not have any moving parts in the water, leading to easier maintenance works. More complete reviews about OWC can be found in [1] and [2].

The hydrodynamic interaction between WECs and sea waves is a complex non-linear process that has being numerically studied using different approaches. Reference [3] developed a theoretical model for a fixed OWC device considering the internal free surface as a weightless piston. Later the models of [4] and [5] considered the deformation of the free surface through the application of the oscillating surface-pressure distribution condition. The numerical models to simulate OWC that can be found in the literature are here summarised in two groups: i) time domain models based on linear water wave theory, and ii) CFD codes based on the integration of the Navier-Stokes equations (meshbased and meshless). Table 1 summarises the main features of the different approaches that will be presented in detail.

TABLE I. NUMERICAL MODELS FOR SOLVING THE DYNAMICS INVOLVED IN WEC ANALYSIS

	Time domain models	CFD models	
		Meshbased CFD	Meshless CFD
Equations	Cummis equation + Linearised hydrodynamic coeffs.	Navier Stokes	Navier Stokes
Method	Boundary Element Method	Finite Volume	Smoothed Particle Hydrodynamics
Viscosity	Inviscid	Viscous	Viscous
Linearity	Linear	Non-linear	Non-linear
Suited for	Low amplitude motions Small oscillations	Viscous losses	Large deformations + Rapidly moving geometries
Efficiency	Fast and efficient	Time consuming + Mesh generation	Very time consuming
Codes	WAMIT, WADAM. WEC-Sim, Nemoh	OpenFoam, IH-Foam, Fluent, REEF3D	DualSPHysics

In the first group, time-domain models based on frequency domain data are usually built upon the Cummins equation ([6]). The Boundary Element Method (BEM) is used to solve the Laplace equation for the velocity potential, which assumes the flow is inviscid, incompressible, and irrotational. BEM was originally formulated for analysing the motions of ships and assumes that all the hydrodynamic forces on a floating body (i.e. wave energy converters) can be modelled using a set of hydrodynamics coefficients. With information of incoming waves as input, BEM computes added masses, the radiation damping coefficients and excitation force coefficients. The movements of the structure (heave, pitch and roll) are obtained from the solution of the frequency-domain or time-domain equations and require information on the sea state and on the PTO. The main advantage of these models is that the codes are very fast and efficient. The problem is that assuming a linear behaviour, WECs cannot be modelled in energetic sea states or close to resonance. The main limitations derive from the small wave amplitude and small motion amplitude assumptions and the incapability to account for real fluid (viscous) effects (boundary layers, turbulence, vortex shedding).

The second main group consists of those models based on the Reynolds Averaged Navier–Stokes (RANS) equations and presents several advantages, not only for solving the velocity field in the whole domain but also for overcoming the limitations of nonlinearity. Thereby, CFD models that approximate Navier–Stokes equations are considered one of the best numerical tools to study the hydrodynamic interaction between waves and WECs. Particularly powerful within this group are those models that include the Volume Of Fluid (VOF) method to capture the movements of the free surface. These models can simulate viscous losses and non-linearities that occur in the interaction between the floating body and the wave train, so that, violent flows with large amplitudes can now be simulated. However, they need an extra algorithm to track free-surface and meshing complex geometries or floating bodies is a hard task. Actually, due to computational requirements, the numerical integration of the RANS equations to model OWC converters was applied, in many cases in the literature, to two-dimensional geometries. The work of [7] carried out a numerical study of an OWC with the commercial CFD code Fluent (also based on finite volumes), investigating the flow distribution in the chamber and the properties of the air-jet impinging on the free-surface. There are many other works using two-phases RANS and VOF models for OWC modelling, but few of them show validation with experimental data. Reference [8] developed a 2D-RANS model to study wave interaction with a semi-submerged OWC chamber and analysed its impact on the energy efficiency. The validation of the model was carried out using the experiments presented by [9]. Some recent works also present the validation of the STAR-CCM+ model in [10] where a RANS-VOF numerical model is used to study the OWC performances for different wave conditions and damping values. The model IH-Foam is also employed in [11] where numerical results of chamber free-surface oscillation and air pressure variation are compared with

experimental data performed in IH-Cantabria. Reference [12] employed Fluent to simulate a heave-only floating OWC including validation against experimental, analytical and other numerical results. Nevertheless, models based on finite volumes present the limitations coming from the meshbased approach to deal with extremely large deformations and rapidly moving geometries.

Although there are many methods based on RANS for wave-structure interaction, including the modelling of floating objects, traditional methods are either meshbased or meshless methods. The meshbased approach solves the equations at fixed nodes in the space. In the meshless description, the positions where equations are solved move with the fluid and a fixed mesh is not used. The meshbased methods (finite elements, finite differences and finite volumes) are currently very robust, well developed and have been applied to a wide range of applications providing highly accurate results. These meshbased methods are ideal for systems where the domain is perfectly defined and for simulations where the boundaries remain fixed. However the creation of the mesh can be very inefficient if the system is complex. In recent years, numerous meshless methods have appeared and grown in popularity as they can be applied to problems that are highly nonlinear in arbitrarily complex geometries and are difficult for mesh-based methods. Within the meshless methods now available, Smoothed Particle Hydrodynamics is, possibly, the most popular and has attained the required level of maturity to be used for engineering purposes.

Hence, SPH is an ideal technique to simulate free-surface flows and presents several advantages compared with meshbased methods to simulate violent wave-structure interaction: i) there is no special treatment to detect the free surface so large deformation can be efficiently treated since there is no mesh distortion, ii) moving complex boundaries and interfaces are easily handled, iii) multiphase flows are simulated without the need of special variables to detect the phases in the space since each individual particle holds material properties of its phase and iv) natural incorporation of coefficient discontinuities and singular forces into the numerical scheme. However, there are few works in literature where SPH is used to simulate wave energy converters. The works of [13] and [14] simulated oscillating wave surge devices and [15] studied point absorber devices but no other works deal with the simulation of oscillating water column using SPH models.

The DualSPHysics code ([16]) is developed by researchers from Universidade de Vigo (Spain) and The University of Manchester (U.K.). DualSPHysics has been developed to use SPH for real engineering problems with software that can be run on either CPUs or GPUs (graphics cards with powerful parallel computing). GPUs offer now a higher computing power than CPUs and they are an affordable option to accelerate SPH with a low economic cost. Thereby, the simulations can be performed using a GPU card installed on a personal computer. In addition, for the purpose of providing a

general model, relevant modes of interaction are not always evident, in which case high spatial and temporal resolutions must be attainable. Furthermore, some simulations may require remarkably large domains. This stresses the need for high performance codes and implementations and it means that DualSPHysics is a perfect candidate since it is the most efficient SPH code worldwide ([17]).

The aim of this paper is the modelling of the hydrodynamic interaction of waves with the OWC device. This part of the procedure provides the input to the energy transfer methods such as air turbines. The DualSPHysics model used to simulate OWC is presented here as a first step towards the modelling of wave energy converters in extreme conditions. The code is first validated with experiments (laboratory scale) of regular waves interacting with a fixed OWC. The model is then applied to simulate a floating OWC device moored to the seabed. Proper wave generation, propagation and active absorption are guaranteed. Chamber free-surface oscillations and the motions and rotation of the floating structure under the action of regular waves are computed. Therefore, DualSPHysics is used to mimic its behaviour in real sea conditions.

II. NEW FUNCTIONALITIES

A. Automatic wave generation

Long-crested waves are generated in DualSPHysics by means of moving boundaries that aim to mimic the movement of a wave-maker as in physical facilities. The wave generation using moving boundary in DualSPHysics consists of piston- and also flap-type wavemakers. A piston-type wavemaker is used in the present study.

First and second order wave generation theories are implemented in DualSPHysics for monochromatic waves. The first order generation is fully described in [18], where generation methods for both monochromatic and random waves are reported. Reference [18] analysed the performance of the wave generation against theoretical results for long-crested waves. For second order wave generation, the reader is referred to the solution proposed by [19] where the author advises to use it only for $HL^2/d^3 < 8\pi/3$, where H and L are the wave height and wavelength respectively (referred to a case of monochromatic waves) and d is the water depth at the wave-maker location in still water conditions. The first order wave generation for monochromatic waves is extended to random waves in DualSPHysics based on the method described in [20]. Two standard wave spectra are implemented and used to generate random waves: JONSWAP and Pierson-Moskowitz spectra. The generation system allows having different random time series with the same significant wave height (H_{m0}) and the same peak period (T_p), just defining different phase seeds.

In this way, wave height, wave period and depth are the key input parameters in DualSPHysics, therefore the time series of wavemaker displacement is computed using the aforementioned wave theory.

B. Active wave absorption for piston-type wave maker

Active wave absorption is used in physical facilities to absorb the reflected waves at the wavemaker in order to avoid that they will be reflected back into the domain. In this way, the active absorption prevents the introduction into the system of extra spurious energy that will bias the results. With active absorption, the position of the wavemaker is corrected every time step.

The active wave absorption system (AWAS) has been implemented in DualSPHysics for a piston-type wavemaker. The technique is based on the approach that appears in [21]. The water surface elevation η at the wavemaker position is used and transformed by an appropriate time-domain filter to obtain a control signal that corrects the piston displacement in order to absorb the reflected waves every time step.

Hence, the target wavemaker position is corrected to avoid reflection at the wavemaker. The position in real time of the wavemaker is obtained through the velocity correction of its motion. For a piston-type wavemaker the velocity correction is calculated using linear long wave theory in shallow water ([21], [22]). For that it is necessary to estimate the free-surface elevation of the reflected waves, η_R , to be absorbed comparing the target incident water surface elevation, η_I , with the measured one in front of the wave-maker, η_{SPH} . The corrected wavemaker velocity is then the summation of velocity correction and the theoretical incident wave-maker velocity. For further details, the reader is referred to [18].

C. Fluid-driven objects

The movement of an object by considering its interaction with fluid particles and using these forces to drive its motion can be also derived in DualSPHysics. This can be achieved by summing the force contributions for an entire body. By assuming that the body is rigid, the net force on each boundary particle is computed according to the sum of the contributions of all surrounding fluid particles according to the designated *kernel* function and smoothing length. Each boundary particle k experiences a force per unit mass given by

$$\mathbf{f}_k = \sum_{a \in WPs} \mathbf{f}_{ka} \quad (1)$$

where \mathbf{f}_{ka} is the force per unit mass exerted by the fluid particle a on the boundary particle k , which is given by

$$m_k \mathbf{f}_{ka} = -m_a \mathbf{f}_{ak} \quad (2)$$

For the motion of the moving body, the basic equations of rigid body dynamics can then be used

$$M \frac{d\mathbf{v}}{dt} = \sum_{k \in BPs} m_k \mathbf{f}_k \quad (3a)$$

$$I \frac{d\boldsymbol{\Omega}}{dt} = \sum_{k \in BPs} m_k (\mathbf{r}_k - \mathbf{R}_0) \times \mathbf{f}_k \quad (3b)$$

where M is the mass of the object, I the moment of inertia, \mathbf{V} the velocity, $\boldsymbol{\Omega}$ the rotational velocity and \mathbf{R}_0 the centre of mass. Eq. 3a and 3b are integrated in time in order to predict the values of \mathbf{V} and $\boldsymbol{\Omega}$ at the beginning of the next time step.

Each boundary particle within the body has a velocity given by

$$\mathbf{u}_k = \mathbf{V} + \mathbf{\Omega} \times (\mathbf{r}_k - \mathbf{R}_0) \quad (4)$$

Finally, the boundary particles within the rigid body are moved by integrating Eq. 4 in time. The works of [23] and [24] showed that this technique conserves both linear and angular momentum.

Validations about buoyancy-driven motion are performed in [25], where the model is tested for solid objects larger than the smallest flow scales and with various densities. Simulations are compared with analytical solutions, other numerical methods and experimental measurements

D. Quasi-static mooring implementation

A new implementation to simulate the behaviour of mooring lines with DualSPHysics is presented in [26]. This new approach allows reproducing the forces on floating bodies, such as vessels, boats, wave energy devices and other off-shore structures moored to the seabed.

A mooring line is a rope, a cable or a chain that holds in position any kind of floating object, more precisely the implementation will be focusing on continuous ropes and wires that can be described by the catenary function (swing moorings). The catenary function refers to the mathematical description of a line with mass hanging between two points. These two points can be at any position relative to each other. The equation that must be satisfied in Cartesian coordinates is $y = \xi \cosh\left(\frac{x}{\xi}\right)$, where y and x are vertical and horizontal coordinates respectively, and ξ corresponds to the form parameter and this parameter shapes the catenary function width.

The maths from the work of [27] is behind this implementation and the solution for the inelastic catenary equations is obtained. In general, the force of the chain corresponds to the proportion of the chain that is lifted. In this way, different conditions for moorings are considered such as the resting chain, partially resting chain, partially extended chain and the fully extended chain.

III. VALIDATIONS

A. Wave generation and absorption

The readers is here referred to the work presented in 10th International SPHERIC Workshop last year in Parma ([18]) where wave generation and wave absorption (passive and active) were presented and validated with analytical solutions and experimental data.

B. Detached OWC chamber

The experiments carried out in the IH-Cantabria wave flume and employed in [28] are used here for the validation of DualSPHysics. The tank was 20.60 m long and the water

depth was of 0.60 m. A cavity open in the bottom to the channel was placed at 5.4 m of the piston to mimic an OWC chamber. A dissipative beach was located at the end of the flume to avoid reflection. Free-surface elevation was measured in the middle of OWC during the physical tests. Figure 1 shows the setup of the numerical tank with the same dimensions as the experimental one.

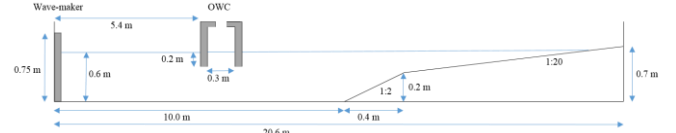


Figure 1. Numerical domain with dimensions of the experiment from Iturrioz et al. (2014).

In this work, there was only access to experimental data of regular waves of $T=3.2$ s, $H=0.08$ m and $d=0.6$ m and with a top opening of 0.05 m. At the scale 1/30 and with a top opening of 50 mm, the effect of the air is negligible for this test, so that the pressure in the OWC air chamber was equal to the atmospheric pressure. Some instants of the simulation with DualSPHysics can be observed in Figure 2. Colour of the particles corresponds to the velocity value.

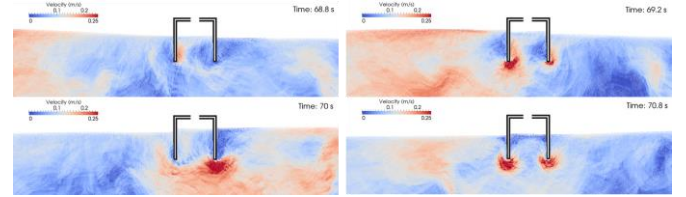


Figure 2. Numerical domain with dimensions of the experiment from Iturrioz et al. (2014).

Figure 3 represents the free-surface elevation measured in the middle of OWC chamber using the time-domain model presented in [28], using IH-Foam (same meshbased CFD model used in [11]) and using DualSPHysics. The water surface elevation measured during the physical model tests is also included for comparison. As expected, SPH numerical results were found to be in better agreement with experimental results than results from the time-domain analysis based on linear water wave theory. It can be observed how DualSPHysics and IH-Foam predict the crests and troughs of free-surface oscillations inside the chamber better than the time-domain model. DualSPHysics and IH-Foam show a similar accuracy for this validation case.

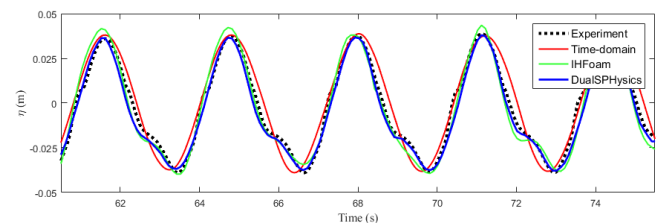


Figure 3. Comparison of experimental data ([28]) with chamber free-surface oscillations obtained using the time-domain model, IH-Foam and DualSPHysics code.

C. Wave interaction with floating bodies

Reference [29] presented success validations of nonlinear water wave interaction with floating bodies in SPH comparing with experimental data that includes deformations in the free-surface due to the presence of floating boxes and the movement of those objects during the experiment (heave, surge and roll displacements). The same validation is also here carried out using DualSPHysics to prove the capability of the model to simulate floating offshore structures. The case studies a floating body under the action of a wave packet. The floating body is a rectangular prism 10 cm long, 5 cm high and 29 cm wide, with density relative to water being 0.68 (680 kg·m⁻³). The mass of the body is 0.986 kg in 3D, but the simulation is performed in 2D. The setup of the experiment is shown in Figure 4. The experiment is better described in [30].

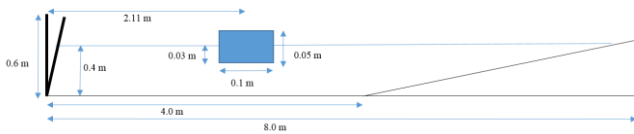


Figure 4. Set-up of the experiment described in [30].

The time history of the flap wavemaker angle used to generate the wave packet is plotted in the first row of Figure 5. At the focusing point the wave packet is quite steep and has a height equal to the body. Then, a nonlinear behaviour is observed in both the resulting wave evolution and the body motion. During the experiments the wave elevation was recorded by two fixed probes, one before the location of the body ($x=1.16\text{m}$) and other after the body ($x=2.66\text{m}$), and the comparison with numerical results is also shown in Figure 5, confirming the correct generation and propagation of the wave packet.

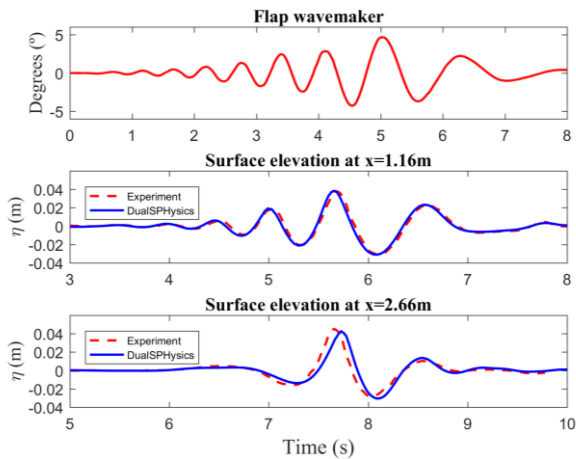


Figure 5. Time history of the flap angle and time series of experimental and numerical free-surface surface elevation.

Figure 6 presents the experimental time series of the floating body motions, heave and sway, compared with numerical results obtained with DualSPHysics, and a good agreement is also observed.

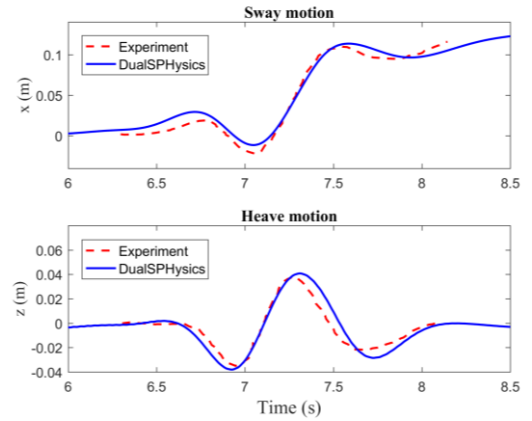


Figure 6. Experimental and numerical time series of the floating body motions (heave and sway).

D. Quasi-static mooring lines

This mooring implementation has been validated with experimental data from [31] and [32] where static experiments were performed for single and multiple lines. The configuration of the chains, the set-up, and the reference data is taken from those.

The first experiment consists of a body with a line attached. The body is moved to different positions relative to the anchoring point in the x direction, all of them at water surface level, and a charge cell provides the value of the tension for the different positions. Figure 7a represents the experiment; the mooring is initially anchored at $x=0\text{m}$ and then is moved from the initial position to sixteen different positions between $x=5.5\text{m}$ and $x=6.4\text{m}$. The second case is used to validate the force exerted on a floating body by two mooring lines. One of the chain is moved from a semi-extended position to a fully lifted position and the other chain increases its resting portion (Figure 7b). The resting position of the object is at $x=0\text{m}$ and chains are anchored at $x=-55\text{m}$ and $x=55\text{m}$. These two chains have the same physical properties.

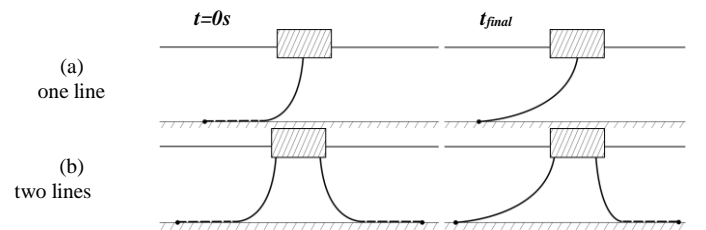


Figure 7. Schematic diagram of the two cases with mooring lines.

Figure 8 (left) shows the horizontal tension for the case of one line. Results obtained with DualSPHysics and the experimental data are in good agreement. Results of the case with two lines are shown also in Figure 8 (right), where the tension of each line (A & B) and the resultant tension from both chains exerted on the body (Merge) are compared with the experimental results. A good agreement is also achieved with the quasi-static approach implemented in DualSPHysics.

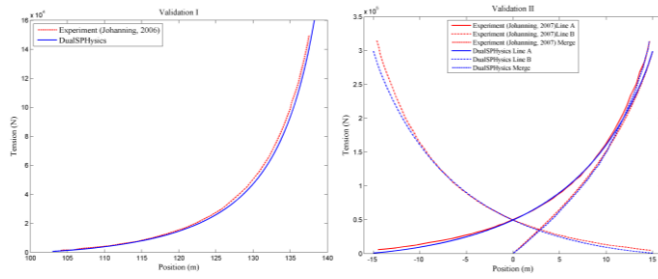


Figure 8. Comparison of experimental horizontal tension with numerical results from DualSPHysics for the two experiments; one line and two lines.

IV. APPLICATION

Once the DualSPHysics code has been validated with experiments in the laboratory, it has been applied to study free-surface oscillations inside the chamber of an offshore floating OWC in the open sea. Note that these cases will be simulated using real dimensions, large domains and long-time events. Therefore, the GPU computing of DualSPHysics makes this SPH code a perfect tool to deal with those simulations that involve millions of particles to be executed at a reasonable time.

As mentioned before, sea waves propagating towards the coast suffer from attenuation, refraction, shoaling and breaking as they approach the shore. In this way, some of the wave power is lost when onshore devices capture wave energy at the shoreline. Floating devices located in the open sea can be a good option but they have to demonstrate their ability to generate power and survive in the most extreme conditions of the ocean. DualSPHysics is a suitable numerical tool to simulate these floating devices in locations with highly non-linear wave movement, severe waves, wave breaking, and overtopping. However, in this numerical simulation, regular non-breaking waves have been simulated in order to obtain preliminary results of free-surface oscillations inside an offshore floating OWC in the open ocean. The geometry and size of the floating OWC represented in Figure 9 have been chosen for computational demonstration purposes rather than as the geometry and size of a realistic device.

Regular non-breaking waves of $H=1.8$ m, $T=9.0$ s, $d=10$ m with $L=81$ m are generated for this preliminary study. In addition, the 3-D numerical tank has been designed to mimic the real situation in the open sea. Therefore, any type of wave reflection should be avoided:

- Passive wave absorption in form of dissipative beach is introduced at the end of the tank.
- Active wave absorption system (AWAS) is used to absorb any reflected wave energy coming from the impact with the external front wall of the floating OWC.
- Open periodic boundaries ([16]) are used instead of lateral solid walls to avoid friction that could difficult the

wave propagation and to avoid any small reflection in the direction perpendicular to the incoming wave direction.

A more complete setup of the numerical domain can be observed in Figure 9 where the dimensions of the tank and the structure can be observed. The channel has a width of 12.8 m and a length of 190 m, being 57 m the distance between the piston and the OWC. The maximum depth is 10 m with a flat region of 80 m and then the beach (8° degrees of slope).

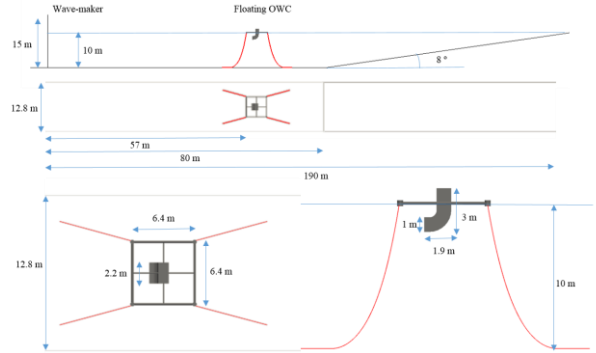


Figure 9. Numerical domain of wave tank and offshore floating OWC.

The floating OWC device is 3 m tall and 2.2 m wide with an opening of 1 m tall. A square floating structure is connected to the device to improve the stability in floatation (section 2.4.3). This floating object is secured to the bottom of the sea by four moored lines and it could be exposed to extreme wave conditions forcing the moorings to work in extreme regimes. Forces of catenary moorings are added to the total force of the floating structure as described in section 2.4.4. The mooring lines have a total length of 14 meters and a wet volumetric density of 7850 kg/m^3 , mimicking the properties of steel wire. A total number of 3,700,000 particles have been created to represent the case under study (being 3,600,000 fluid particles, 2,000 floating particles representing the OWC and arms and the rest the boundaries of the system). A physical time of 60 seconds was simulated during 51 hours using GeForce GTX TITAN.

Figure 10 plots different instants of the simulation. Colour of the surface indicates the velocity field. By modelling only regular non-breaking waves with the use of an active wave absorption system, a regular pattern of surface oscillations inside the chamber is achieved. Figure 11 represents the wave surface elevation measured in the middle point of the chamber, where a certain repeatability is observed. Starting from 20 seconds, regular cycles are measured in the chamber. Note that the shaded area of the figure tries to identify one of these cycles, which also corresponds to the instants shown in Figure 10.

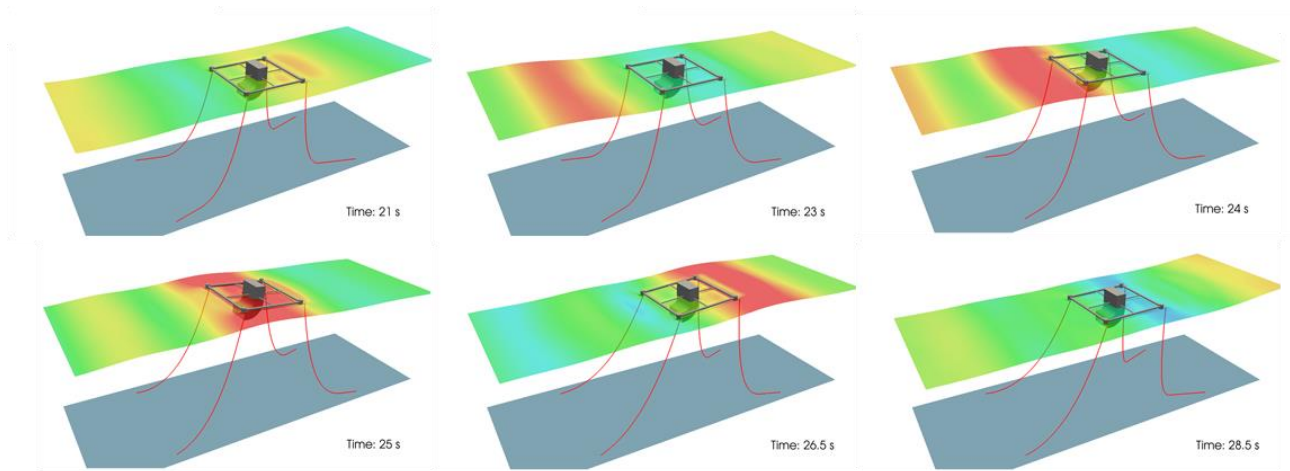


Figure 10. Different instants of the simulation with floating OWC in the open sea.

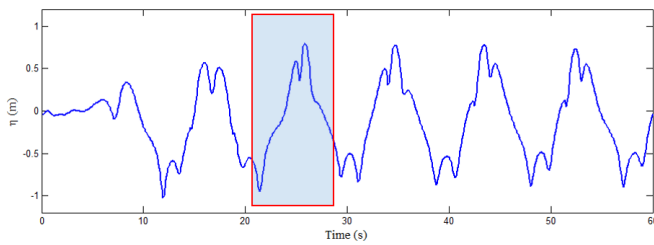


Figure 11. Free-surface oscillations inside the floating OWC chamber.

The numerical time histories of the motions of the floating structure are shown in Figure 12. The surge and heave components present simple harmonic oscillations, while small sway motion in the lateral direction can be seen. This is thanks to the role of the catenary moorings that limit the displacement of the floating structure. In this way, the OWC is always aligned with the direction of the incident waves (roll and yaw angles are negligible). Moreover, the motions are reduced in order to get a correct vertical position of the water column inside the chamber which will facilitate the operation of the OWC to maximise the energy.

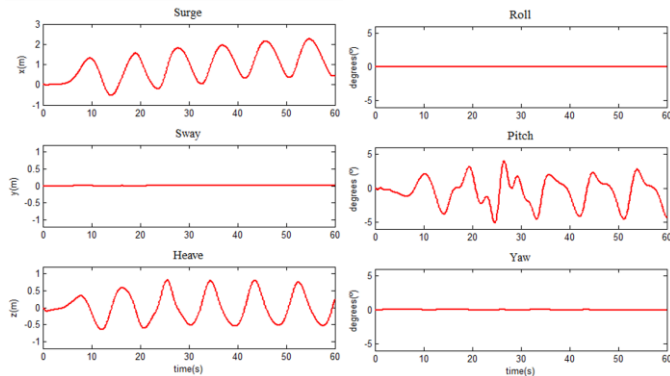


Figure 12. Time histories of the motions of the floating OWC (surge, sway and heave motion, and roll, pitch and yaw rotation).

V. CONCLUSIONS AND FUTURE WORK

The DualSPHysics SPH-based model is presented in this work as a suitable tool to simulate offshore floating OWC devices. SPH is a meshless numerical model that deals easily with high non-linearities and large deformation of the free surface. DualSPHysics is implemented to exploit the parallel computing power of GPUs so the millions of particles required to simulate real complex geometries and domains can be simulated at a reasonable computational time. These features make the code ideal to simulate floating WEC devices under the action of extreme waves, including wave breaking and overtopping, in order to study their survival capacity and efficiency to absorb the available wave energy. As far as we know, this paper presents the first validation of a fixed detached OWC device with SPH, and the first SPH simulation of a floating OWC moored to the seabed where free-surface oscillations inside the chamber are computed.

Free-surface oscillations inside the OWC chamber are computed using the numerical code DualSPHysics and compared with physical data from experiments performed at the IH Cantabria wave flume. A good agreement is observed and a convergence study is also shown.

DualSPHysics is then applied to one case of study. A floating OWC device is designed including a structure with arms that helps in the floatation and to keep a vertical position of the water column inside the chamber. Passive and active wave absorption systems are also employed to mimic the state of the open sea and catenary moorings help to reduce the heave, surge and roll motion of the floating device. Free-surface oscillations are also successfully computed using DualSPHysics. It is important to mention that only regular waves have been simulated, but the DualSPHysics allows simulating any sea state starting from standard spectra, which is more significant for practical applications. Furthermore, only long-crested waves are simulated but, as future work, the generation of short-crested waves will be implemented.

The effect of the air is important at these scales and should have been simulated to obtain realistic results, however in this first implementation, only the fluid phase is solved. Future work will be first focused on the simulation of the air phase inside the OWC chamber using other versions of DualSPHysics considering water-air phases ([33]).

ACKNOWLEDGEMENT

This work was partially financed by Xunta de Galicia under project “Programa de Consolidación e Estructuración de Unidades de Investigación Competitivas (Grupos de Referencia Competitiva)”. The authors gratefully acknowledge the support of NVIDIA Corporation with the donation of the GTX Tesla K40 GPU used for this research. This study was also supported in part with computational resources at the Barcelona Supercomputing Center under the activity FI-2015-2-0008.

REFERENCES

- [1] Heath, T.V., 2012. A review of oscillating water column. *Philos. Trans. R. Soc. A* 370, 235–45.
- [2] Falcão, A.F.O., Henriques, J.C.C., 2016. Oscillating-water-column wave energy converters and air turbines: A review. *Renew Energy* 85, 1391–1424.
- [3] Evans, D.V., 1978. The oscillating water column wave energy converters. *Journal of the Institute of Mathematics and its Applications* 22, 423–433.
- [4] Evans, D.V., 1982. Wave power absorption by systems of oscillating surface pressure distributions. *Journal Fluid Mechanics* 114, 481–499.
- [5] Sarmento, A., Falcão, A.F.O., 1985. Wave generation by an oscillating surface-pressure and its application in wave-energy extraction. *Journal of Fluid Mechanics* 150, 467–485.
- [6] Cummis, W.E., 1962. The impulse response function and ship motions. *Schiffstechnik* 9, 101–109.
- [7] Paixão Conde, J.M., Gato, L.M.C., 2008. Numerical study of the air-flow in an oscillating water column wave energy converter. *Renewable Energy* 33, 2637–44.
- [8] Zhang, Y., Zou, Q.P., Greaves, D., 2012. Air–water two phase flow modelling of Hydrodynamic performance of an oscillating water column device. *Renewable Energy* 41, 159–170.
- [9] Morris-Thomas, M.T., Irvin, R.J., Thiagarajan, K.P., 2007. An investigation into the Hydrodynamic efficiency of an oscillating water column. *Journal of Offshore Mechanics and Arctic Engineering* 129, 273–278.
- [10] López, I., Pereiras, B., Castro, F., Iglesias, G., 2014. Optimisation of turbine-induced damping for an OWC wave energy converter using a RANS-VOF numerical model. *Applied Energy* 127, 105–114.
- [11] Iturrioz, A., Guanche, R., Lara, J.L., Vidal, C., Losada, I.J., 2015. Validation of OpenFOAM for Oscillating Water Column three-dimensional modelling. *Ocean Engineering* 107, 222–236.
- [12] Luo, Y., Wang, Z., Peng, G., Xiao, Y., Zhai, L., Liu, X., Zhang, Q., 2014. Numerical simulation of a heave-only floating OWC (oscillating water column) device. *Energy* 76, 799–806.
- [13] Rafiee, A., Elsaesser, B., Dias, F., 2013. Numerical simulation of wave interaction with an oscillating wave surge converter. *Proceedings ASME 32nd International Conference on Ocean, Offshore and Arctic Engineering*.
- [14] Edge, B., Gamiel, K., Dalrymple, R.A., Herault, A., Bilotta, G., 2014. Application of gpusph to design of wave energy. *Proceedings of the 9th SPHERIC International Workshop*, Paris, France.
- [15] Yeylaghi, S., Moa, B., Beatty, S., Buckham, B., Oshkai, P., Crawford, C., 2015. SPH Modeling of Hydrodynamic Loads on a Point Absorber Wave Energy Converter Hull. *Proceedings of the 11th European Wave and Tidal Energy Conference (EWTEC2015)*, Nantes, France.
- [16] Crespo, A.J.C., Domínguez, J.M., Rogers, B.D., Gómez-Gesteira, M., Longshaw, S., Canelas, R., Vacondio, R., Barreiro, A., García-Feal, O., 2015. DualSPHysics: open-source parallel CFD solver on Smoothed Particle Hydrodynamics (SPH). *Computer Physics Communications* 187, 204–216.
- [17] Domínguez, J.M., Crespo, A.J.C., Valdez-Balderas, D., Rogers, B.D., Gómez-Gesteira, M., 2013. New multi-GPU implementation for Smoothed Particle Hydrodynamics on heterogeneous clusters. *Computer Physics Communications* 184, 1848–1860.
- [18] Altomare, C., Suzuki, T., Domínguez, J.M., Barreiro, A., Crespo, A.J.C., Gómez-Gesteira, M., 2015. Numerical wave dynamics using Lagrangian approach: wave generation and passive & active wave absorption. *Proceedings of the 10th SPHERIC International Workshop*, Parma, Italy.
- [19] Madsen, O.S., 1971. On the generation of long waves. *Journal of Geophysical Research* 76(36), 8672–8683.
- [20] Liu, Z., Frigaard, P., 2001. Generation and Analysis of Random Waves. *Laboratoriet for Hydraulik og Havnebygning, Institutet for Vand, Jord og Miljøteknik, Aalborg Universitet*.
- [21] Shaffer, H.A., Klopman, G., 2000. Review of Multidirectional Active Wave Absorption Methods. *Journal of Waterway, Port, Coastal and Ocean Engineering* 126, 88–97.
- [22] Didier, E., Neves, M.G., 2001. A Semi-Infinite Numerical Wave Flume Using Smoothed Particle Hydrodynamics. *International Journal of Offshore and Polar Engineering* 22(3), 193–199.
- [23] Monaghan, J.J., Kos, A., Issa, A., 2003. Fluid motion generated by impact. *Journal of Waterway Port, Coastal and Ocean Engineering* 129, 250–259.
- [24] Monaghan, J.J., 2005. Smoothed Particle Hydrodynamics. *Rep. Prog. Phys.* 68, 1703–1759.
- [25] Canelas, R.B., Domínguez, J.M., Crespo, A.J.C., Gómez-Gesteira, M., Ferreira, R.M.L., 2015. A Smooth Particle Hydrodynamics discretization for the modelling of free surface flows and rigid body dynamics. *International Journal for Numerical Methods in Fluids* 78, 581–593.
- [26] Barreiro, A., 2015. Smoothed Particle Hydrodynamics model for civil and coastal engineering applications [PhD Thesis]. *Universidade de Vigo, Spain*.
- [27] Faltinsen, O.M., 1993. *Sea Loads on Ships and Offshore Structures*, Cambridge University Press.
- [28] Iturrioz, A., Guanche, R., Armesto, J.A., Alves, M.A., Vidal, C., Losada, I.J., 2014. Time-domain modeling of a fixed detached oscillating water column towards a floating multi-chamber device. *Ocean Engineering* 76, 65–74.
- [29] Bouscasse, B., Colagrossi, A., Marrone, S., Antuono, M., 2013. Nonlinear water wave interaction with floating bodies in SPH. *Journal of Fluids and Structures* 42, 112–129.
- [30] Hădžić I, Hennig J, Peric M, Xing-Kaeding Y (2005). Computation of flow-induced motion of floating bodies. *Applied Mathematical Modelling* 29, 1196–1210.
- [31] Johanning, L., Smith, G.H., Wolfram, J., 2006. Mooring design approach for wave energy converters. *Proceedings of the Institution of Mechanical Engineers, Part M: Journal of Engineering for the Maritime Environment* 220(4), pp. 159–174.
- [32] Johanning, L., Smith, G.H., Wolfram, J., 2007. Measurements of static and dynamic mooring line damping and their importance for floating WEC devices. *Ocean Engineering* 34, 1918–1934.
- [33] Mokos, A., Rogers, B.D., Stansby, P.K., Domínguez, J.M., 2015. Multi-phase SPH modelling of violent hydrodynamics on GPUs. *Computer Physics Communications* 196, 304–316.